MODELING AND OPTIMIZING MIXING EFFICIENCY IN A TWO-IMPELLER STIRRED TANK

By

SHU YANG

A thesis submitted to the

Graduate School-New Brunswick

Rutgers, The State University of New Jersey

In partial fulfillment of the requirements

For the degree of

Master of Science

Graduate Program in Chemical and Biochemical Engineering

Written under the direction of

Marianthi, G. Ierapetritou

And approved by

_____

_____

_____

New Brunswick, New Jersey

October, 2017

ABSTRACT OF THE THESIS

Modeling and Optimizing Mixing Efficiency in a Two-Impeller Stirred Tank

by SHU YANG

Thesis Director:

Dr. Marianthi, G. Ierapetritou

For commercial scale reactors, insufficient mixing is a common phenomenon. Imperfect mixing can have significant impact on product quality. Therefore, improving the efficiency of mixing is an important part of process design and optimization. This study intends to develop a computationally feasible model of a stirred tank reactor, and use this model to improve the mixing efficiency. In this study, a scaled-down version of a real stirred tank reactor is modelled. A computational fluid dynamics (CFD) based compartmental model was developed through finite volume discretization of mass balance equation. A resolution sensitivity test was conducted to determine the discretization mesh scheme. This model demands less computation than dynamic CFD simulation while shows satisfactory predictive power. A benchmark chemical reaction system was integrated to characterize the mixing efficiency, which is composed of a first-order decay and a parallel second order coupling. Two operating policies were studied to optimize the mixing efficiency. The first is a static policy which employs a constant feeding rate in a semi-batch process, and the second is a dynamic policy which adjusts the feeding rate dynamically. Feeding point and feeding rate profile are the decision variables. Mixed-

integer surrogate optimization was implemented to find the optimum, and the solution was validated with interior point method. The results obtained indicate that the choice of feeding point is independent of feeding rate profile. Additionally, it has been concluded that the static policy results in poor utilization of feed. By implementing the dynamic policy, through the extra degree of freedom, the waste of material is reduced and improvement in the economy of process is achieved.

Acknowledgement

I would never be able to finish my master's study without the guidance of my committee members, advice from industry, help from my friends, and support from my family.

I would like to express my deepest gratitude to my advisor, Dr. Marianthi, G. Ierapetritou for her professional guidance and support of my study and research. Her patience, motivation, and immense knowledge help and encourage me to overcome a lot of problems I met during my research. I would like to thank my committee members Dr. San Kiang and Dr. Ioannis P. Androulakis for their interest in my work.

I would also like to thank Dr. Kiang and Dr. Lai for their invaluable guidance from the industrial perspective. Their broad knowledge and insightful view helped realized important issues which give me a sense of direction.

My sincere thanks to all my friends who supported me during my time in the US. I am grateful for the help from Parham who offers me numerous ideas and discussions on my research all the time. I especially appreciate Zilong, Sebastian, Nirupa, Lisia, Abhay, Atharv and Ou who make the graduate life at Rutgers colorful.

Last but not the least, I would like to thank my parents for their continuous support and guidance throughout my life.

Table of Contents

List of Illustrations

Chapter 1: Introduction

Stirred tank reactors (STRs) are widely used in chemical industry and pharmaceutical industry. They provide excellent mixing performance for gas dispersion, solid suspension and chemical reactions. Flow in STRs are created by interaction between the rotating impellers and the stationary baffles. Fluid is driven around by the impellers, and deformed by the shear created by impellers and baffles. Both affect the mixing process, and show substantial influence on the course of chemical reaction. Traditional design of STRs are based on the assumption of perfect mixing. However, in cases where the time scale of reactions are smaller than that of mixing, the efficiency of mixing should be taken into consideration. Perfect mixing assumption can be justified in bench-scale device since strong agitation can be provided inside a small vessel. However, for commercial scale reactors, where technical-economical performance should be taken into consideration, this assumption cannot be justified. The deviation from perfect mixing models can lead to severe damage to product quality[1]. Mixing is an important factor in process design.

Mixing inside STRs is categorized according to their characteristic length scales: the first category is driven by convection, which has length scale higher than the inertial subrange, usually referred to as macro-mixing[2]. The second category is driven by coarse-scale turbulent exchange, which has a length scale larger than Kolmogorov scale, usually referred to as meso-mixing[3]. Finally, the third category is driven by viscous-convective deformation and the following molecular diffusion, which has a smaller length scale than Batchelor scale; commonly described as micro-mixing[4].

Different categories of mixing contributes to the course of chemical process differently. To understand the states of mixing and the associate impact, their characteristic time scales should be compared to that of chemical reactions. For macro-mixing the characteristic time scale is of the order of one second, while for micro-mixing, it's around 10^{-2} seconds[5]. It can be concluded that the most desired state of mixing, which is well macro-mixing and well micro-mixing, may only be feasible for slow reaction systems. Moreover, partial segregation can be easily encountered in systems with fast kinetics.

The mechanism of different mixing category are different. Considering variations in length and time scales, first principle model of mixing is numerically infeasible. Similar to the case with turbulence, direct simulation is infeasible with current computational resources. Moreover, modeling micro-mixing relies on the information of turbulence, therefore the difficulties in modeling turbulence is inherited in micro-mixing models. In addition, for the discretization of space required in numerical simulations of turbulent flow, the grid size defined by the discretization method is larger than the characteristic length scale of micro-mixing. As a result, micro-mixing models are formulated as a source term in the mass balance equation instead of the flux term.

The early researches of mixing majorly focused on micro-mixing. Models developed include multi-environmental model[6], engulfment-deformation-diffusion model[7], and interaction by exchange with mean model[8]. Nevertheless, limited description of the bulk flow field was included, which accounts for the efficiency of macro-mixing. Considering the characteristic time scale of micro and macro mixing, for industrial reactors partial segregation caused by insufficient macro-mixing is more likely to happen. To deal with this problem, compartmental models are developed to describe the macro-mixing

efficiency in reactors. The fluid body in the reactor is modelled with a matrix of interconnecting cells[9]. Each cells inside the matrix is modelled as perfect reactors. The bulk velocity profile of certain reactor configuration was determined by experiments, which was used to calculate the flow throughput of each cell. Network of Zones model[9] is developed based on the idea of compartmental modeling. The radially dominant flow driven by a Rushton turbine is captured, and the distribution of chemical species is solved. For situations where the flow pattern is simple, assumptions could be made based on the preliminary understanding, and the mass transfer process could be quantified with flow numbers[10]. Improvement of compartmental model was introduced later by integrating Stocks-Einstein equation to describe the streamline profile[11]. A stochastic switching mechanism was introduced to account for the influence of turbulence, which contributes to the species shifting between different streamlines. Multiple models were developed to further improve compartmental mixing models[10, 12], but its incapability to deal with complex flow still limit the implementation of compartmental mixing model.

With the development of computers, Computational Fluid Dynamics (CFD) has become a good alternative. With CFD, robust solutions of the bulk flow field is available with limited time and economical cost. CFD based mixing models, which combines CFD with chemical kinetics models has been widely adopted. Good predictive power has been achieved in the work of multiple-time-scale turbulent mixer model[13], finite-mode probability density function[14], direct quadrature method of moments combining with the interaction by exchange with the mean micro-mixing model(DQMOM-IEM)[15], and finite-rate/eddy-dissipation(FR/ED) model[16]. Although some models have parameters determined by experiments, CFD-based mixing model in general do not require

experimental input or preliminary knowledge of the flow pattern. As a result, CFD-based mixing model is more robust and its predictive power is not compromised with complex flow field.

With the wide adoption of CFD-based mixing model, CFD-based optimization frameworks were implemented to optimize the mixing process. CFD models were developed for quench reactor[17], heat exchangers[18], cyclone separator[19], and combustion chamber[20]. Good results are achieved, and this integrated framework has shown its potential as a promising design method. In these works, evolutionary algorithms are widely adopted. Genetic Algorithm (GA) was implemented in the work with quench reactor and heat exchangers [17, 18]. Artificial Neural Networks (ANNs) was used together with GA in the work with cyclone separator[19]. Through the implementation of evolutionary optimization algorithm, no assumptions about the nature of the models are needed, which make the adaptation easy.

However, evolutionary algorithms are relatively inefficient, because a significant amount of function evaluations are required, which further increase the computational expense. In the work with quench reactor, which has a four-dimensional design space, 2000 function evaluations were performed. Each function evaluation included a CFD simulation, which takes around 182 minutes on a 20-core server for each individual simulation[17]. The overall computational expense is prohibitive.

Moreover, considering the complex nature of reactive flow, models with higher complexity are required in many processes. Probability density function model is adopted to model chemical reactions where different phases are generated[21]. To model the precipitation process inside a STR[22, 23], adopting population balance equations has become

the standard method to predict the particle size distribution. To replace the empirical model of mass flux, E-model was developed[4] in which the interested chemical species were modelled with a pseudo phase and its distribution is tracked with the volume of fluid (VOF) simulation. Despite the significant improvement these models have achieved, the corresponding computational expense also increase significantly. As a result, the integrated CFD-based optimization framework could be computationally prohibitive, which limited its wide implementation.

Instead of replacing compartmental models with CFD simulations, many researchers are trying to make full use of both methods, and CFD-based compartmental models are developed. In this method, CFD is implemented to provide a prediction of the flow field, which is later used to model the mass flux in compartmental model. Comparing to experimentally measuring the flow field, CFD simulation is more cost and time efficient. Moreover, without a need for preliminary knowledge of the flow field, reactors with complex flow field could also be easily modelled while still maintaining accuracy and robustness. On the other hand, comparing to direct CFD simulations, because the Navier-Stocks equation is replaced with a system of simple ordinary differential equations (ODE), CFD-based compartmental model is significantly cheaper computationally.

With the listed advantages, CFD-based compartmental model is becoming more and more popular in providing computationally cheap description for chemical processes. Wide applications are seen in modeling crystallizers. In crystallizers where flow patterns has a huge influence on the resulting particle size distribution (PSD), mixing has been the focus of research. Previously, Computational Fluid Dynamics- Population Balance Equations (CFD-PBE) model was the standard tool for predicting industrial-scale crystallizers[22, 24, 25].

However, considering the computational cost of this simulation, a CFD-based compartmental model was developed[14]. This CFD-based compartmental model accounts for the hydrodynamics, and PBE is integrated to keep track of the growth of particles. This model is computationally cheaper and good predictive power has been achieved.

Considering the computationally expensive methods of previous work in CFD-based optimization, CFD-based compartmental model could be a good alternative. In this project, we developed a CFD-based compartmental model to describe the mixing process inside reactors. A more efficient optimization algorithm is implemented to solve for the optimal operating policy. This method can significantly save the computational time and providing easy interface.

Chapter 2: Modeling Mixing Process

2.1 Objectives

Mixing plays an important role in industrial processes, in this project we'll develop an integrated model of mixing process, including both the flow pattern and chemical kinetics. Considering the realities in industry, we are more interested in certain situations and some simplifications are done accordingly. In industry, many processes are conducted at the vendor site, and designing the reactor would be unnecessary. For simplification purpose, designing the geometry of the reactor is not in the scope of this project. Moreover, considering that many reactions are conducted in solutions, the dilute solution simplifications could be made. Comparing to gas reactions happening in combustion engines, the course of reaction in liquid solution don't have a significant influence on the overall flow pattern. Despite that strong exothermic process could influencing the density of fluid and in turn influence the flow pattern, comparing to the turbulent flow created by the impeller, this influence is still not significant. With these ideas in mind, in this work the reaction kinetics and flow pattern would be decoupled and solved separately.

Based on the listed simplifications, model structure is determined. Description of macro-mixing is based on the bulk convection predicted by CFD. Meso-mixing is also simplified into the convective term. After CFD-based bulk flow pattern is solved, micro-mixing model and chemical kinetics models are coupled. With this structure, the great variation in time and length scale can be effectively treated. In addition, with this decoupled structure, we don't have to re-solve the flow field if we make alterations to the kinetics.

2.2 Model development

Mixing is driven by the mass transfer process, the first principle equation is implemented to describe the mixing process,

$$\frac{\partial C_i}{\partial \mathrm{t}} = -\nabla \cdot \boldsymbol{N}_i + R_i \tag{1}$$

Where C_i represents the concentration of chemical species i, N_i represents the mass flux of species i, while $R_i$is the source term for species i.

The flux term and the source term are both function of time, concentration and space. To make it feasible for numerical solution, some derivation based on the assumptions made in the beginning of this chapter should be performed.

2.2.1 Discretization

We discretized the fluid body in space to allow numerical solution. Similar to current CFD software packages, Finite Volume Method (FVM) is adopted. In the case with CFD, momentum conservation equation is discretized and studied. This method could be implemented in arbitrary geometry while remaining robust. Moreover, balance of flux between different control volumes is guaranteed throughout the discretization process. Through the implementation of the Gauss Divergence Theorem, integrals are done at the surface instead of the whole volume, which automatically guaranteed conservation at the surface between different control volumes. In addition, FVM gives good prediction even without adequate functional framework[26]. Considering these properties, FVM is widely adopted in fluid mechanics, semi-conductor simulation and heat transfer, where flux is important.

Before discretizing the mass balance equation, a mesh T of domain Ω over which the conservation law is to be studied is introduced. K is an element of mesh T which is an open subset of domain Ω, called a control volume. The structure of mesh T is an important step of this discretization method, and it relies heavily on the conservation equation.

The principle of FVM is to discretize equations in space according to the defined mesh. Variables are assigned at each control volume to represent the space distribution. With each variable one equation is written. The derivative of the variables at each discretization point is replace by finite difference.

In this project, mass balance equation of chemical species is studied. With finite volume method, the 'volume averaged' concentration $\overline{C_i}$ is assigned as the unknown variable for every control volume. A volume integral is taken for each control volume:

$$\int_{\boldsymbol{K}_i} \frac{\partial C_i}{\partial t} + \int_{\boldsymbol{K}_i} \nabla \cdot \boldsymbol{N}_i = \int_{\boldsymbol{K}_i} R_{\boldsymbol{K}_i} \tag{2}$$

Where the concentration profile C_i is replaced with the volume-averaged concentration $\overline{C_i}$ for every control volume. The partial differential equation (PDE) used to describe mass transfer is replaced with a set of ODEs. Moreover, with the divergence theorem, the flux term is calculated with a surface integral:

$$V_i \frac{d\overline{C_i}}{dt} + \oint_{S_i} \boldsymbol{N}_i \cdot \boldsymbol{n} dS = \int_{\boldsymbol{K}_i} R_{\boldsymbol{K}_i} \tag{3}$$

Where n is the unit normal vector of surface S_i, pointing outwards from control volume K_i, V_i is the volume of K_i.

In the framework of FVM, the space distribution of variable inside each control volume is ignored. The flux term and source term should also be transformed into functions of the volume averaged concentration.

2.2.2 Mass flux modeling

To solve the discretized ODE system, the flux term across the boundaries should be modelled as a function of volume averaged concentration $\overline{C_i}$. The mass flux in fluid system is described with:

$$\boldsymbol{N} = C\boldsymbol{v} + \boldsymbol{J} \tag{4}$$

Where v is mass averaged flow velocity, and J is the molar flux relative to the mass averaged velocity of the mixture. The mass averaged velocity is derived from continuity equation, and is solved together with the conservation of momentum. Diffusion term J is described with Fick's law for dilute solution with constant density. However, the diffusion term may vary for different systems at different length scale. Specifically for this project, the bulk flow inside a stirred tank has high Reynolds number, leading to turbulent flow. Within the turbulent flow regime, mass flux is dominated by the mass-averaged velocity term and the diffusion terms is negligible on the macro-scale. Although mass diffusion J is significant on micro-mixing, its length scale is below the mesh. As a result, to capture it with mass flux in current discretization method is infeasible. According to our model framework, we will leave the diffusion effect to the micro-mixing model which is integrated later.

$$\boldsymbol{N} = C\boldsymbol{v} \tag{5}$$

Based on the assumption that the course of reaction has no influence on the flow field, we can decouple the reaction kinetics from the bulk flow pattern. The mass-average velocity $\boldsymbol{v}$ is independent from $\overline{C_i}$ and we could study them separately. The velocity field $\boldsymbol{v}$ should be calculated first.

Turbulent flow is an unsteady complex process, which means that the velocity field v is a function of time. To model turbulent flow is a critical area for any engineering field that involves CFD. The most common way to deal with this complex problem is by solving for the time-averaged solution. This method is called Reynolds-averaged Navier–Stokes equations (RANS). It requires less computational resources comparing to Eddy Simulation, while remaining good precision unless it involved separation or large recirculating regions. In this work, the time-averaged velocity field is solved to model the mass flux. This adaptation is justified since the unsteadiness is not severe in stirred tanks. Moreover, our operating time is longer comparing to the characteristic time scale of unsteady eddies. Given that velocity field is no longer dependent on time, it's calculated in priority as the constant coefficient in the ODE system. For simplicity, we write it as $F_{i,j}$, describing the flux from control volume i to control volume j.

$$V_i \frac{d\overline{C_i}}{dt} + \sum_j F_{j,i}\overline{C_j} - \overline{C_i}\sum_k F_{i,k} = \int_{\boldsymbol{K}_i} R_{\boldsymbol{K}_i} \tag{6}$$

In order to determine the velocity field and in turn determine $F_{i,j}$, CFD is adopted to export the velocity field which is independent from the kinetics. Since the same mass-average velocity is used to solve for the conservation of momentum, it's justified to solve for the flux term from the momentum conservation equation in CFD simulation. The flux

term $F_{j,i}$ is the surface integral of the velocity field over the interface between different control volumes.

$$F_{i,j} = \int_{S_{i,j}} \boldsymbol{v} \cdot \boldsymbol{n} dS \tag{7}$$

When surface integral is calculated numerically, some alteration to the finite volume method should be done. In standard finite volume method, the flux is solved together with momentum equation, continuity equation and energy equation with the same mesh. This treatment ignored the distribution of concentration inside the control volume, and the surface integral is replaced with multiplication. However, in reality, the distribution of concentration on the control volume surface is important. In fluid bodies, strong circulation could present between two different control volumes, which contributes strongly to mass transfer. If we take the surface integral without considering the distribution on the surface, the circulation is evened out, which will introduce significant error.

Alteration applied in this project is based on the decoupling of flow and kinetics. Other than solving the mass-flux together with momentum equation and continuity equation with the same mesh, the velocity term could be exported from CFD simulation, where a much finer mesh is used. With this method, the sub-cell information is captured and the flux is defined as such so we could capture the turbulent exchange between different zones:

$$F_{i,j} = \sum_{S_{i,j}} \boldsymbol{\psi}(\boldsymbol{v} \cdot \boldsymbol{n}) \, \Delta S$$

Where

$$\boldsymbol{\psi}(\mathrm{x}) = \begin{cases} 0, & \mathrm{x} < 0 \\ \mathrm{x}, & \mathrm{x} \geq 0 \end{cases} \tag{8}$$

2.2.3 Source modeling

Now that the flux term is defined, we need to model the source term to close the equations. In finite volume method, we are ignoring sub-control volume informations. Underlying this method is the idea of homogeneous reaction inside each control volume.

$$\int_{\boldsymbol{K}_i} R_{\boldsymbol{K}_i} = V_i R_{\boldsymbol{K}_i} \tag{9}$$

Chemical reactions and micro-mixing which have smaller length scale than the mesh should be modeled in the source term. In this work, chemical kinetics is modelled with rate law:

$$\boldsymbol{R}_{V_i} = \sum_r k_r \prod_j [C_{j,r}]^{\eta_{j,r}} \tag{10}$$

Where $\eta_{j,r}$ is the rate exponents of species j in reaction r, while k is the rate constant of reaction r.

Micro-mixing is defined with EDD models:

$$\boldsymbol{R}_{V_i} = \frac{C_{\boldsymbol{\phi}}}{2}\frac{\varepsilon}{k} \tag{11}$$

Where $C_{\boldsymbol{\phi}}$ is the mechanical time to scalar time ratio, which is a function of local Reynolds number. ε is the turbulent dissipation rate, and k is the turbulent kinetic energy. Although turbulent dissipation rate and turbulent kinetic energy cannot be directly measured, these parameters can be exported from turbulent model in CFD simulation.

In the source term, semi-batch addition of chemicals should also be considered.

$$\boldsymbol{R}_{V_i} = \boldsymbol{\delta}_{i,p} F_{feed} C_{feed} \tag{12}$$

Where i stands for control volume i, while p stands for feed zone p. $\boldsymbol{\delta}_{i,p}$ is the Kronecker delta.

With this modeling framework, we can easily integrate different kinetics and micro-mixing models. In cases where rate law and EDD model fails to give satisfactory precision, population balance equations and VOF simulation can also be incorporated [22].

2.2.4 Integrated mixing model

Based on the models developed for different processes, integrated mixing model could be built. The way they are integrated is based on the mechanism of the process itself. The process of semi-batch addition happens in parallel to micro-mixing and chemical reaction, so it should be integrated by addition. However, in the case with micro-mixing and chemical reaction, better agreement with the experimental data has been achieved if different processes are considered to happen in serial[16]. If mixing happens faster than chemical reactions, the overall performance is dominated by kinetics, and vice versa. With this consideration, source term is governed by the slower process. The integrated model for the mass balance of chemical species is built. It's a system of ODEs which could be used to solve for the concentration profile, and further implemented for optimization.

$$V_i \frac{d\overline{C_i}}{dt} + \sum_j F_{j,i}\overline{C_j} - \overline{C_i}\sum_k F_{i,k} = \boldsymbol{Min}\left\{V_i \sum_r k_r \prod_k \left[\overline{C_{k,r}}\right]^{\eta_{k,r}}, \frac{C_{\boldsymbol{\phi}}}{2}\frac{\varepsilon}{k}\right\} + \boldsymbol{\delta}_{i,p} F_{feed} C_{feed} \qquad (13)$$

2.2.5 Resolution sensitivity test

Based on finite volume method, mass balance equation is discretized into control volumes. The complex PDE is replaced by a set of ODEs. However, underlying this method lies the assumption of homogeneity inside each control volume. Behavior of medium in this model should exhibit higher diffusivity than the true medium. This deviation is called numerical diffusion.

Deviation caused by numerical diffusion is determined by the system being modelled and the type of discretization that is used. Heuristically, with higher resolution mesh, the discretized model should behave more like the continuous reality. However, with increasing resolution, the size of the ODE system also increases, which may lead to higher computational expense. In addition, with the increasing resolution, the size of each control volume is decreasing, which may lead to an increasing stiffness of the whole system.

To deal with this problem, a resolution sensitivity test is implemented to find the optimal resolution for the mesh. In this method, the integrated model is tested with different resolutions. If the output of this model is no longer changing significantly with the increasing resolution, the model can be viewed as insensitive to resolution. With this method, we could determine the lowest resolution that gives acceptable precision.

This test is kinetic sensitive, and should be run with the integrated model. If the system has slow chemical reactions, perfect mixing assumption could be adopted, without hurting the predictive power, which is essentially only using one control volume. However, for fast reaction, the deviation caused by numerical diffusion could be significant, which would require higher resolution. Although for different kinetics we can use the same flow field data from CFD, if a new kinetics is adopted, the resolution sensitivity test should be re-

conducted with the updated integrated model. The flowchart in Figure 1 displays how this method works.

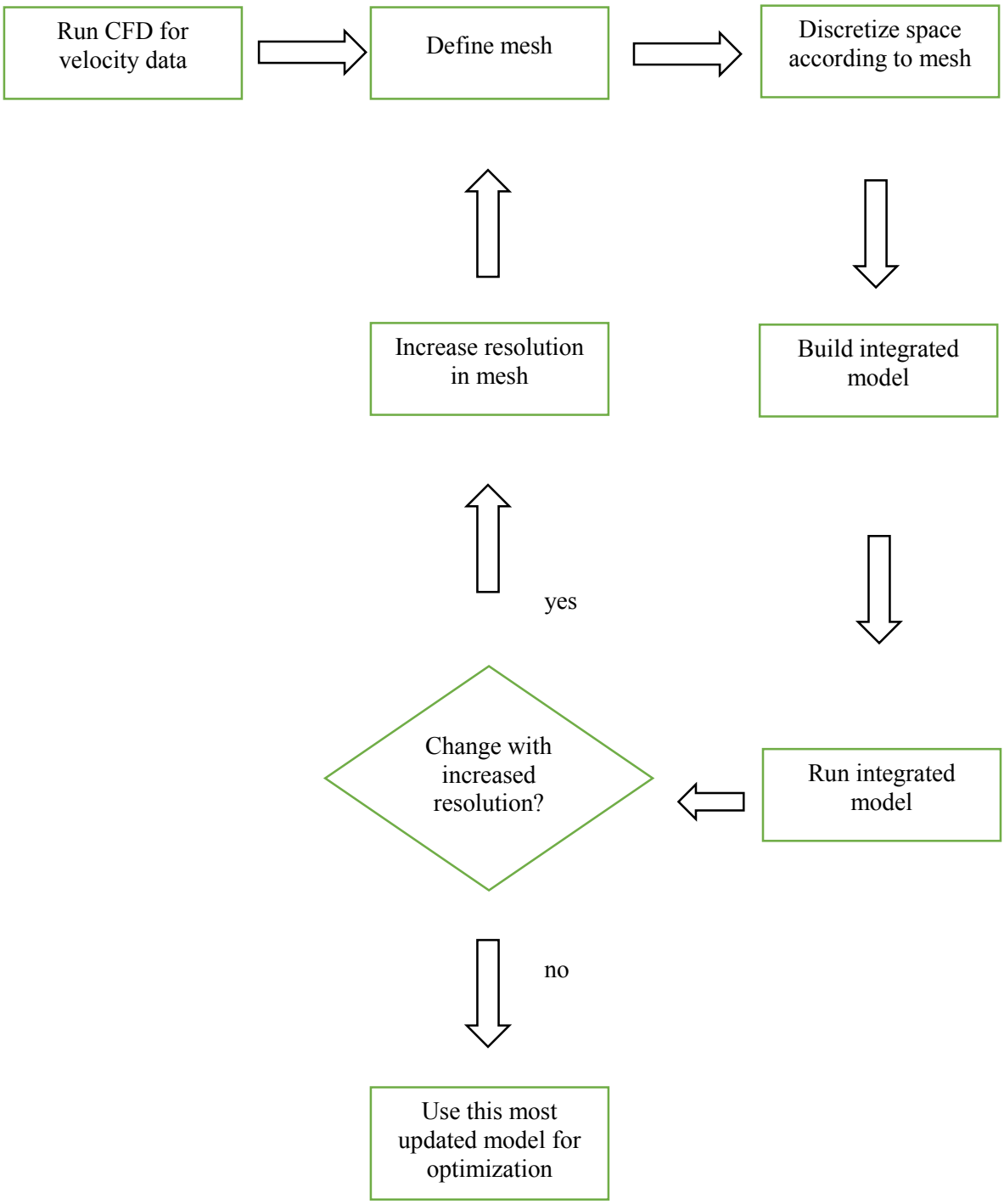

Figure 1. Flowchart of resolution sensitivity test

Chapter 3: Case study

With this model development framework from chapter 2, we'll model a scaled-down version of a real industrial stirred tank reactor as a case study, which would later be used to solve for the optimal operating policy. A benchmark reaction system for mixing efficiency is integrated in this work so the performance of mixing can be characterized. In this chapter, an integrated mixing model is developed based on the properties of the reactor and the reaction system. The developed model is then validated through the resolution sensitivity test.

3.1 Reaction system

Reaction system used in this project is a famous pair of parallel competitive reactions. This reaction system is composed of a first-order decay and a parallel second order coupling.

$$A \xrightarrow{k_1} S \tag{14}$$

$$A + B \xrightarrow{k_2} R. \tag{15}$$

Where A is a diazonium salt (diazotized 2-chloro-4-nitroaniline) and B is pyrazolone (4-sulphophenyl-3-carboxypyrazol-5-one). R the desirable product, which is a dyestuff and S is the unwanted product of decomposition[10]. Since first order reaction is not sensitive to mixing, and is only dependent on Residence Time Distribution (RTD) [27]. The first-order decaying is added as a characterization of time, serving as the clock inside the reactor. The rate constant of this reaction system is $k_1=10^{-3}s^{-1}$ at a PH of 6.6 at 40℃, and k_2 is 7000m^3 $kmol^{-1}$ $s^{-1.}$ This reaction is chosen so that the characteristic time scale of this reaction system

is similar to that of macro-mixing. The logic is that influence of macro-mixing is most significant when the characteristic time scale of macro-mixing is at the same order as that of chemical reactions. The same logic holds for Bourne reaction for micro-mixing, both have a characteristic time scale several orders of magnitude lower than that of macro-mixing [7].

Considering the characteristic time scale of kinetics and micro-mixing, we can see that in this chosen process, micro-mixing is dominated by chemical reactions. Since micro-mixing and chemical reaction happen in a serial manner, micro-mixing model could be removed from this integrated model.

$$V_i \frac{d\overline{C_i}}{dt} + \sum_j F_{j,i}\overline{C_j} - \overline{C_i}\sum_k F_{i,k} = V_i \sum_r k_r \prod_k \left[\overline{C_{k,r}}\right]^{\eta_{k,r}} + \boldsymbol{\delta}_{i,p} F_{feed} C_{feed} \qquad (16)$$

With this reaction system, selectivity of side product can be chosen as a quantitative index for the effect of macro-mixing. With better macro-mixing performance, more R could be produced with less A consumed.

3.2 Reactor setup

A 74L fully baffled stirred tank is chosen to study its macro-mixing performance. The inner diameter is 0.5m and the liquid height is 0.4m. The agitation system has two impellers. The one on the bottom is a Rushton impeller with a diameter of 0.2m and an offset from bottom of 0.1m. The upper impeller is a pitched blade turbine (PBT) with a diameter of 0.2 and is place above Rushton impeller with an offset of 0.14m. The blade angle of the PBT is 45°. The direction of rotation is set up in a way that PBT is driving fluid downwards to

the Rushton impeller. The agitation speed is chosen to be 60rpm, which is derived from a real process from industry. Structure of this reactor is shown in Figure 2.

Both reactants are dissolved in aqueous solution. The stirred tank is initially charged with pyrazolone (B) solution with a concentration of 6×10^{-5}M. Diazo (A) solution is added into the stirred tank in a semi-batch manner, the concentration of which is 7.4×10^{-2}M. This set up is adopted from the original design in the literature [9].

Considering that if the feeding rate is infinitely slow, high selectivity can be reached regardless of the efficiency of macro-mixing. The time span of this process should be defined reasonably so the influence of macro-mixing is highlighted. In this work, considering the characteristic time scale of macro-mixing, the time span of this process is set as 150s.

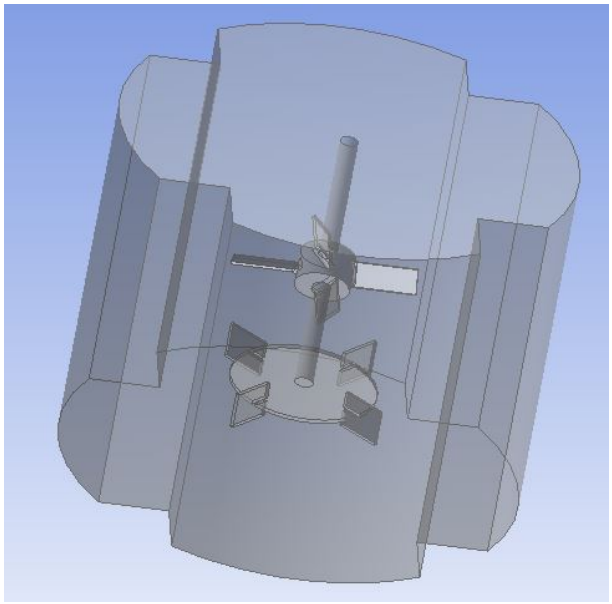

Figure 2. Geometry of the two-impeller stirred tank

3.3 CFD simulation

CFD simulation on this reactor is adopted to solve for velocity field. This simulation only needs to be run once and can be integrated with different chemical reactions and operating policies. In that way the model is computationally cheaper without hurting the accuracy.

Although pyrazolone solution is fed in a semi-batch manner into the stirred tank, the influence of the feeding pipe over the flow pattern is ignored. A simulation without feeding is done with the same set up. Based on the simulation result, each control volume defined during model development has a volumetric flow rate at the order of 0.1L/S. However, the volumetric flow rate of feeding is at the order of 1×10^{-3}L/S. Since the flow rate of feeding is significantly smaller than that of the bulk flow inside the reactor, influence of feeding over the flow pattern is ignored.

In CFD simulation, a steady state solution is solved with the commercial code of Fluent 16.0. With this code, the Reynolds-Averaged-Navier-Stocks (RANS) equation was numerically solved with multi-reference frame (MRF) method. To close the equations, k-epsilon turbulence model with standard wall functions was adopted. The velocity field is shown in Figure 3.

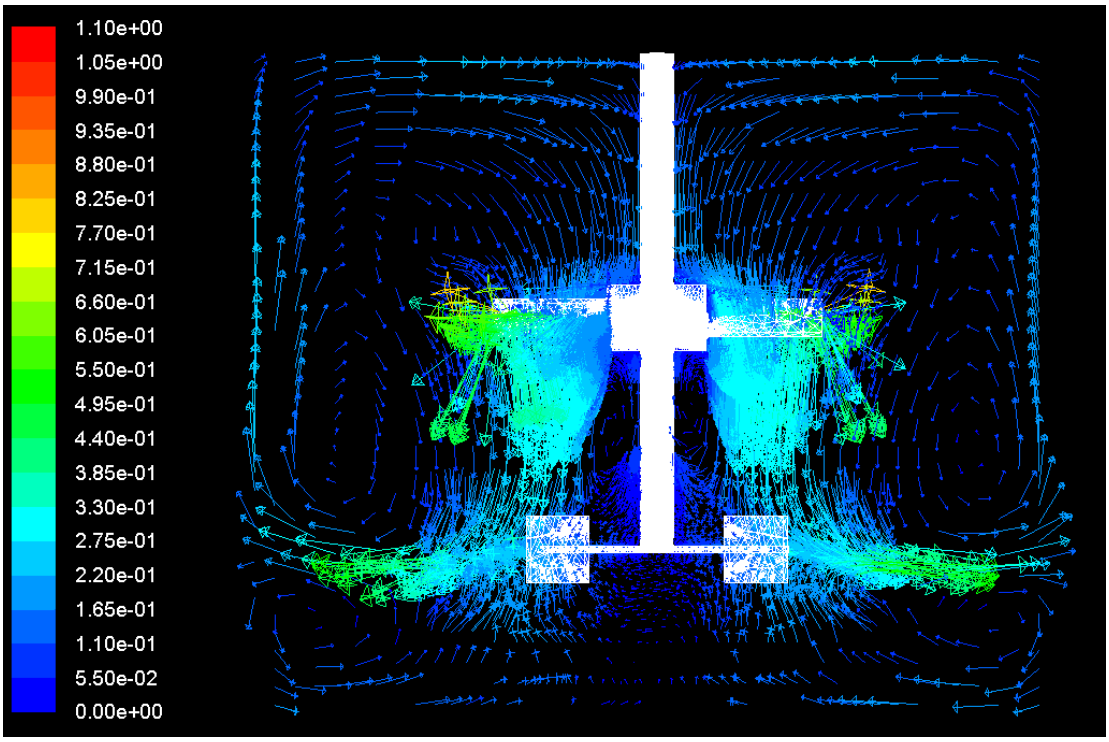

Figure 3. Vector plot of velocity field inside the stirred tank

3.4 Discretization

The mesh is defined by evenly dividing the reactor in radial, axial and tangential directions. The discretization of the mass balance equation is proceeded according to the mesh defined. With the results from CFD simulation, the unknown parameters for the discretized mass balance equation could be defined.

$$V_i \frac{d\overline{C_i}}{dt} + \sum_j F_{j,i}\overline{C_j} - \overline{C_i}\sum_k F_{i,k} = V_i \sum_r k_r \prod_k \left[\overline{C_{k,r}}\right]^{\eta_{k,r}} + \boldsymbol{\delta}_{i,p} F_{feed} C_{feed} \qquad (17)$$

Where V_i for each control volume is defined by the mesh, $F_{i,j}$ can be determined by the velocity field from CFD simulation. With this closed set of ODEs, the concentration profile could be solved in time.

3.5 Resolution sensitivity test

Resolution sensitivity test is done in an iterative manner for each discretization scheme. Considering that different addition point is adopted for different operating policy, theoretically every possible addition point should be tested before implementing this model for optimization. In this work, seven samples are taken inside the reactor to represent all possible choice of addition points. If the chemical reaction trajectory no longer change for every sample point with respect to increased resolution, this model is considered as no longer sensitive to resolution. The seven sample points are, above PBT, PBT tip, between PBT and Rushton, at Rushton tip, below Rushton, the corner of the reactor and behind baffle. Considering the slow dynamic of this reaction system, the number of control volumes is initially set as 504 and gradually increase. By comparing the concentration trajectory of different species in time, we can see that 640 control volumes is the least refined mesh when the model is no longer sensitive to resolution. Comparing to the trajectory with 704 and 768 control volumes, no significant difference has been witnessed. In Figure 4, the trajectory of concentration of A when the addition point is at the corner is displayed.

Through resolution sensitivity test, discretization scheme with 640 control volumes is chosen. The discretized reactor is shown in Figure 5. It has 8 segments in the radial direction, 10 segments in the height direction and 8 segments in the tangential direction. All control volumes are indexed with a 3-d vector, in the format of [radial index, axial index, tangential index].

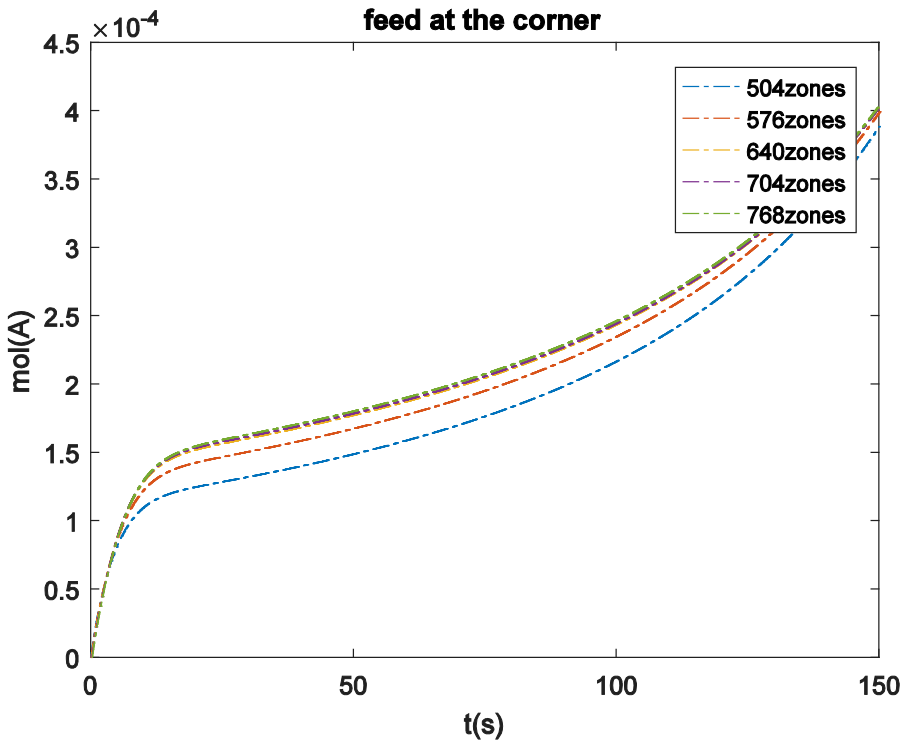

Figure 4. Trajectory of species A for (a) 504 cells (b) 576 cells (c) 640 cells (d) 704 cells (e) 768 cells. The addition point is at the corner of STR

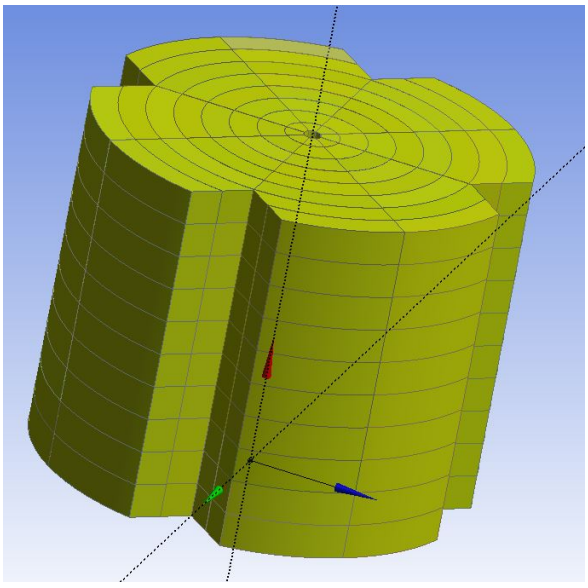

Figure 5. Final mesh adopted in this project

Chapter 4: Static Operating Policy Optimization

4.1 Problem formulation

With the integrated model, space variation of chemical concentration could be captured. Unlike the situation in ideal reactors, the route of reaction depends not only on the feeding rate, but also on the feeding point of reagents. For simple reactor geometries with single impeller, generally the feeding point is chosen at the tip of the impeller. However, for reactors with more complex setup, the best addition point is no longer obvious. With this integrated model, however, we could easily set up the feeding point and study its influence on the chemical process. In Figure 6, the influence of addition point is displayed. In that plot two addition point is studied, one is at the corner of the reactor, which has an index of [7, 0, 2], the other one is at the pitched blade tip, which has an index of [4, 4, 3].

Through the comparison between trajectories of different addition points, influence of addition point over chemical process is pronounced. Reagents added at the corner of the reactor is not distributed well inside the stirred tank, and the overall progress of chemical reaction is slowed down. It's reasonable to take addition point into the design space. Underlying the discretization framework, each control volume is treated as homogeneous. Different choices of addition point would behave exactly the same if they are in the same cell. So the control volume where the feeding point lies could be chosen as the variable that defines the addition point.

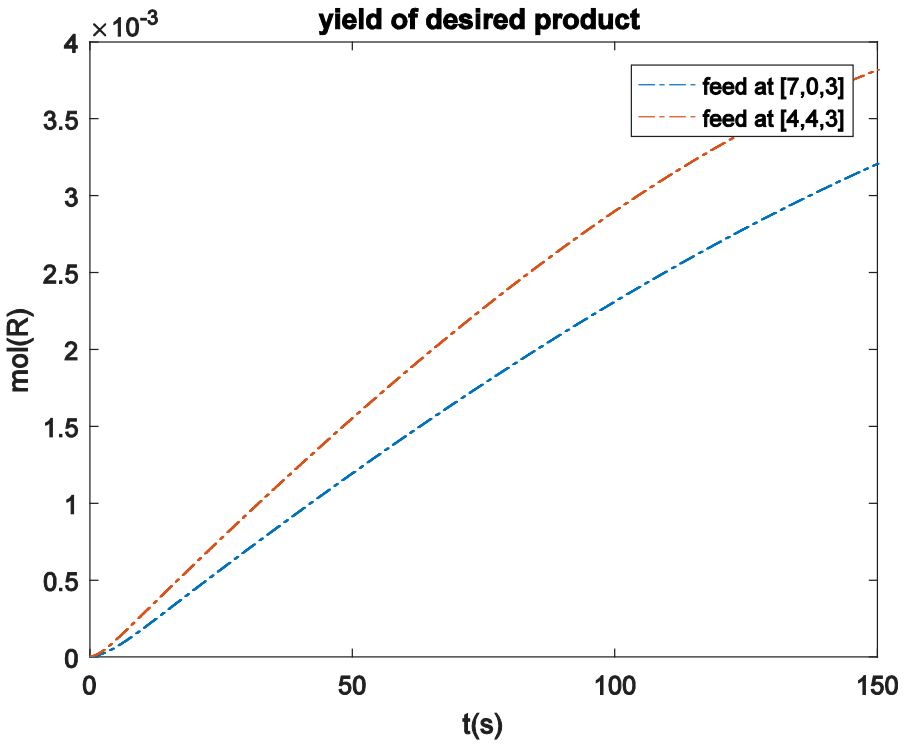

Figure 6. Trajectory of the desired product yield when then addition rate is at (a) corner of STR ([7,0,3]) (b) tip of Rushton turbine ([4,4,3])

The objective is to optimize the macro-mixing performance. Instead of defining a multi-objective optimization problem, two factors are considered into one terms. In experiments, macro-mixing is characterized by the selectivity of the side product, which is used to characterize different reactors with identical feeding rate. However, this method would fail if it's used to characterize different feeding rate in the same reactor, since the selectivity index would always prefer slow feeding. In this project, a new index is adopted based on real life situations. For a chemical process, it's preferred that more product is made with less raw material fed. Our objective function is defined in the form of revenue, assuming the worth of R is ten time as that of A. With this set up, we could formulate the problem

that maximize the performance of the reactor by choosing the best feeding point and feeding rate.

$$Max \qquad (10y_R - y_A) \tag{18}$$

subject to

$$[y_R, y_A] = \boldsymbol{\varphi}(r, a, t, f) \tag{19}$$

$$r, t \in [0,7] \tag{20}$$

$$a \in [0,9] \tag{21}$$

$$f \in [0,2] \tag{22}$$

Where y_R denotes the yield of R, and y_A denotes the amount of A fed. r, a and t are integer variables that defines the control volume in which the feeding pipe lies. f denotes the feeding rate of A, which has a unit of 0.1ml/s. $\boldsymbol{\varphi}(r, a, t, f)$ is the 150s simulation run with the model developed in last chapter.

4.2 Mixed integer surrogate optimization

The formulated optimization problem has both integer and continuous decision variables, and it is categorized as mixed-integer optimization problems. These problems can be easily found in engineering, planning and portfolio management, and are in general NP-hard. The methods proposed to solve mixed-integer problems have two major groups, branch and bound method, and evolutionary strategies.

Branch and bound method is currently the most universally adopted method to solve mixed-integer optimization problems, first proposed in 1960 [28]. This method is based on two major steps, branching and bounding. In branching step, the candidate points are recursively divided into sub-sets. All sub-sets are arranged in the form of a rooted tree, with the full set at the root. In the bounding step, each nodes in the rooted tree is bounded by solving a relaxed problem. Based on the upper and lower bound solved in the bounding step, nodes which can't produce better results comparing to the best solution so far is discarded.

Evolutionary strategy is inspired by reproduction, mutation, recombination and selection, which are natural processes in biology. The mechanism is based on the idea that through mutation, crossover and selection of individuals and their offspring, the whole population evolves and better individuals can be found. Offspring are generated through mutation and crossover, so this method is able to get out from local optimum and approach global optimum. This approach is widely applied in engineering, art, biology and economy. The reason for this wide application lies in the fact that this method don't require any assumption about the nature of the problem, so it could be easily implemented even without sufficient knowledge of the system.

The problem we are trying to solve has some special properties other than mixed-integer decision variables, which brings many difficulties. First of all, evaluation of objective function is computationally expensive since it requires running a simulation based on the integrated mixing model. Moreover, the simulation is based on an ODE solver, in which the decision variables serves as the parameter. As a result, this model can only be treated

as a black-box. In addition, to relax the integer constrains that defines addition zone is not theoretically sound.

Based on the properties of this problem, the implementation of branch and bound is not feasible. Since the evaluation of objective function is expensive, the bounding step is computationally prohibitive. Moreover, the integer constraints can't be relaxed, so solving for the upper and lower bound would require mixed-integer solvers. These properties also prohibits the adoption of evolutionary strategies. Comparing to other optimization algorithms, evolutionary strategies requires more function evaluations. Since the evaluation of function is expensive, evolutionary algorithm would require prohibitive computational resources.

Currently, surrogate based optimization has been the focus in global optimization research. Its ability to find global optimum has been proven and it has become a promising field in derivative-free optimization algorithms. Comparing to classical optimization methods which is based on calculating derivatives analytically or numerically, this method searches for optimizer based on the surrogate model instead of derivatives. This property has made this method successful with black-box models, where calculating the derivatives numerically requires a significant amount of function evaluations. Moreover, with surrogate model, both local and global search is included, which makes it possible to get out of local optimum and reaches global optimum. For classical optimization algorithms, however, searching based solely on derivatives or first order optimality will be trapped in local optimum. On the other hand, comparing to evolutionary strategies, surrogate optimization is more effective. Unlike evolutionary algorithms, surrogate optimization can find global optimum with significantly less function evaluation.

Surrogate optimization works in an iterative manner. In the initial step, a certain number of sampling point is chosen by random sampling or other sampling strategies. Based on the function evaluation at chosen sample points, an initial surrogate model is built. Based on the initial surrogate model, new sampling points are chosen by solving an auxiliary problem which evaluates the surrogate model. The auxiliary problem is defined as maximizing the expected improvement [29], or minimizing the bumpiness[30]. At new sampling point, a function evaluation of the computationally expensive model is done and the surrogate model is updated. This process is conducted iteratively until a stopping criteria is met, and the best point so far is returned.

Although surrogate optimization is successful in solving optimization problems with continuous decision variables, limited work has been done in solving mixed-integer problem. Difficulties arise when faced with integer decision variables. Since solving auxiliary problem is the key step in surrogate optimization, with integer variables, the auxiliary problem became a mixed-integer optimization problem. Considering the huge increase of computational expense when integer variables are introduced, solving the auxiliary problem is no longer computationally cheap. Moreover, since the surrogate model may not be unimodal, global optimization should be implemented when solving the auxiliary problem, which would further increase the computational expense.

Available works in surrogate optimization with integer variables are [31, 32], both uses radial basis function (RBF) to build the surrogate model. In Holmstrom's work[31], the commercial TOMLAB optimization environment is integrated, and the auxiliary problem is solved with mixed-integer sub-solvers provided in this environment. With this method, constrains are added as a penalty term in objective function, which requires careful

treatment of the penalty term. In Müller's work[33], auxiliary problem is no longer defined as an optimization problem. Instead, a random sampling strategy is implemented, where a random sequence of sampling points are chosen, and evaluated based on the surrogate model. Certain scores are assigned to each points based on the surrogate evaluation and the next sampling point is determined based on the scores. In this method no commercial code is required and according to the author, the performance is satisfactory comparing to other methods. In our project, this method is chosen to solve for the optimizer.

Before adopting this method for solving the optimization problem, how this method deal with feasibility should be discussed. Since the model is computationally expensive to evaluate, the feasibility analysis based on function evaluation would further increase the computational burden. To deal with this difficulty, effective methods have been proposed that build an extra surrogate model for the feasibility problem [34]. However, in current work, the feasibility problem is considered in a simpler manner. During updating the surrogate model with new sampling points, the constraints are checked. If the sampling point is infeasible, the worst value plus a penalty is assigned to this point and the surrogate model is updated with this penalized value. This method would discourage sampling near the infeasible regions. However, if the feasible region is scarce, or many infeasible points are sampled, the surrogate model might be distorted and fail to give a good prediction about the optimizer.

Considering this limitation, the implementation of this method should be cautious. In current project, the only constraints are boxed constraint without requiring evaluation of this computationally expensive model. So in this work, the implementation could be

justified. But in cases where feasibility analysis is not trivial, improvement should be done before this method could be implemented.

4.3 Results and discussion

Considering the properties of this optimization problem, mixed integer surrogate optimization algorithm is adopted. The cubic radial basis function is chosen to build the surrogate model. Initial sampling points are selected with Latin Hypercube Sampling and the algorithm would stop after 500 function evaluation. Shown in Figure 7 is the progress plot. After 50 function evaluation the algorithm has found the optimizer, which is efficient.

The optimal addition policy favors the addition at the Rushton turbine region. Comparing to the pitched blade region or the region in the middle. Feeding at Rushton turbine region can distribute materials more effectively and produce more desired product with less reagents added. The optimal feeding rate is 5.39258x10-4L/s. With this feeding policy, the reaction trajectory for different chemical species are plotted in Figure 8, 9 and 10.

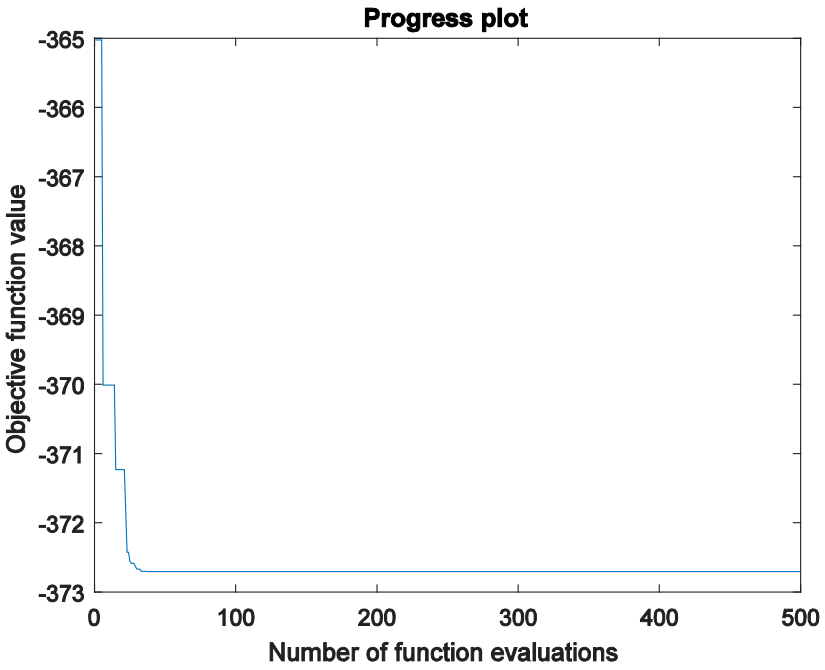

Figure 7. Progress of MISO solver towards the optimizer

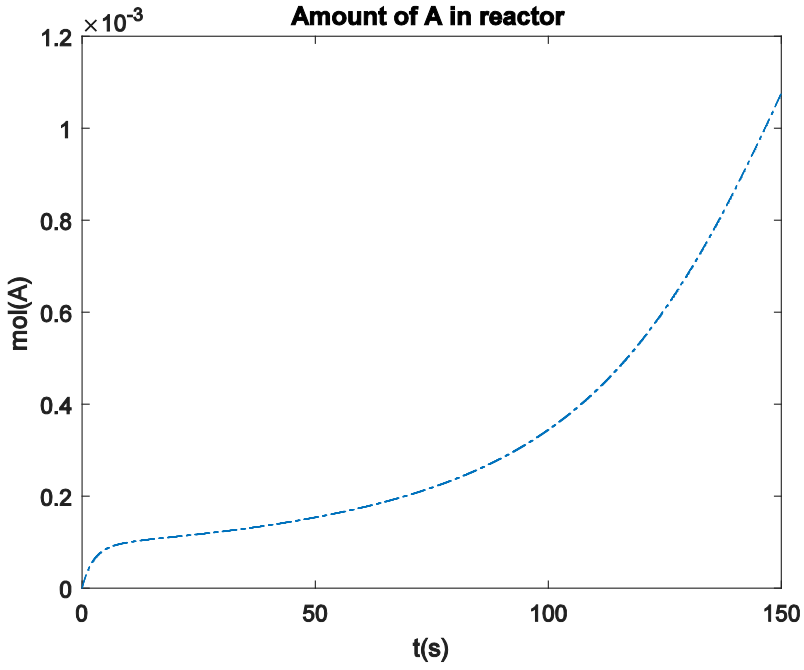

Figure 8. Trajectory of species A under the optimal static operating policy

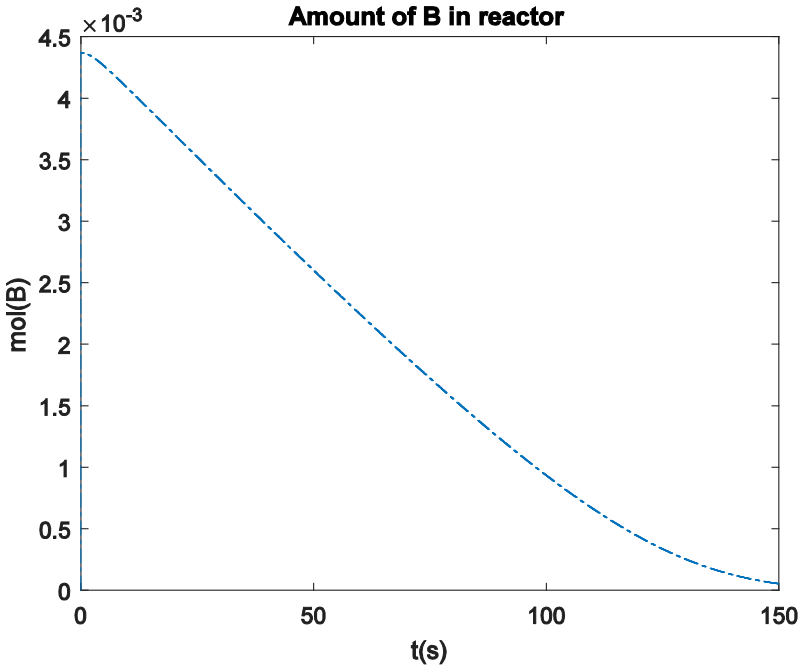

Figure 9. Trajectory of species B under the optimal static operating policy

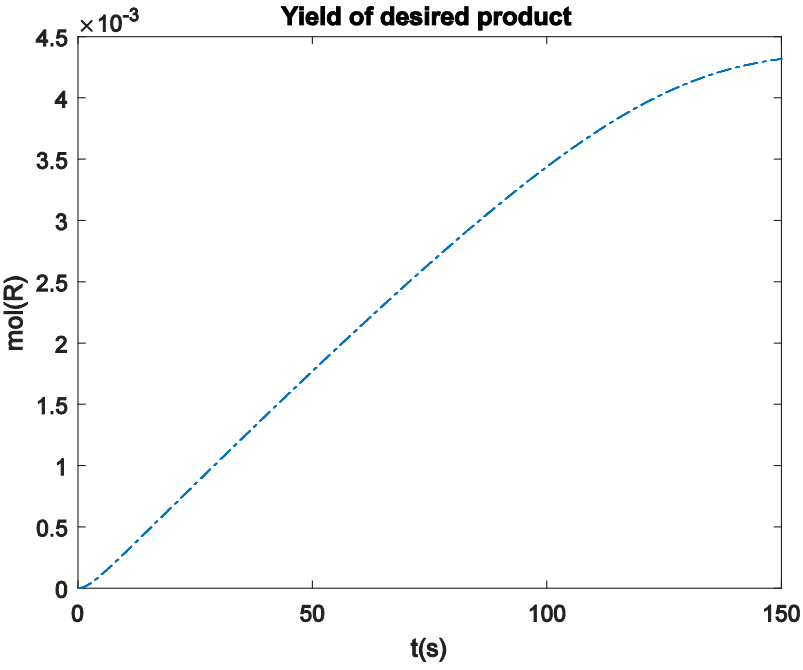

Figure 10. Trajectory of desired product under the optimal static operating policy

As the trajectory of A suggested, when the process ended, amount of A presenting in the system is at the highest level. This is reasonable since the reactant is feeding with a constant rate. With consumption of B, A would be accumulated faster. However, this accumulation would lead to a waste of reagents and compromise the economic performance. So constant feeding is not the optimal option. Since the concentration of B is decreasing in time, the feeding rate should also be decreasing in time for better performance.

Chapter 5: Dynamic Operating Policy Optimization

5.1 Problem formulation

Considering the waste of reactants when adopting a constant feeding strategy, a dynamic feeding strategy could be used. By tailoring addition rate with respect to time, higher degree of freedom is available to further optimize the feeding policy. In this chapter an optimization problem would be formulated aiming to produce more desired product with less reagents fed. In this dynamic feeding policy, the whole operating time is divided into N_p discrete feeding stages. In each feeding stages feeding rate is kept constant, but the feeding rate varies for different feeding stages. Time span of each feeding stage and the corresponding feeding rate are the decision variables that defines the feeding policy. Considering that the best addition point is not highly dependent on the addition rate, addition point is no longer in the scope of this problem and the best addition point found from last chapter is adopted. The optimal stage length and feeding rate will be determined by solving the following optimization problem.

$$Max \qquad (10y_R - y_A) \tag{23}$$

subject to

$$[y_R, y_A] = \boldsymbol{\varphi}\left(t_1, f_1, t_2, f_2, \dots, t_{N_p}, f_{N_p}\right) \tag{24}$$

$$\sum t_i = 150, \qquad i = 1, \dots, N_p \tag{25}$$

$$f_i \in [0,2], \qquad \forall i = 1, \dots, N_p \tag{26}$$

$$t_i \geq 0, \qquad \forall i = 1, \dots, N_p \tag{27}$$

The objective function is defined in the same way as the last chapter, which is in the form of revenue. Time span of each feeding stage i is defined with the variables t_i, and the corresponding feeding rate is defined with variable f_i. The first constraint specifies that the time span of the whole process is 150s. The remaining are lower and upper bound of the decision variables. In here the number of stages N_p is treated as a parameter instead of a variable. Considering the higher degree of freedom more stages would provide, a larger stage number would always be preferred. In addition, it's difficult to penalize the increase of stage numbers, so it's not in the scope of this project. Instead, an increased number of addition stages is tested and it would stop when an increased addition policy don't lead to a significantly improvement in operating policy.

To solve this optimization problem, interior point method is chosen. In this method constrains are treated with barrier functions, and the Karush–Kuhn–Tucker (KKT) conditions is numerically solved to get the optimizer. Since KKT is only the necessary but not sufficient condition for optimizer, this method is a local solver and different starting point should be tested. The nonlinear optimization toolbox provided by Matlab is chosen to numerically solve this problem.

5.2 Result discussion

The optimization problem is numerically solved for single feeding stage (constant feeding), two-stage feeding and three-stage feeding. Single stage feeding works as a way to validate the optimizer of the static addition policy. Two-stage and three-stage feeding policy are also solved, and significant improvement from the constant feeding policy is achieved. Since no significant improvement has been found comparing the three-stage and

two-stage policies, the two-stage policy is finally adopted. The best feeding rate found for the constant feeding policy is 5.4370x10^{-4}L/s, which agrees well with the optimizer found by the mixed integer surrogate optimization algorithm. From this result, we can conclude that the mixed-integer surrogate optimization algorithm gives satisfactory results. The best two-stage feeding policy found with this optimization solver is to start feeding at 16.3532x10^{-4}L/s for 43.0005s, followed by 106.9995s feeding at the rate of 0.0366x10^{-4}L/s. The three stage feeding policy is solved in the same manner, and the best feeding policy is a 8.5097s stage feeding at 37.1512x10^{-4}L/s, followed by a 33.3592s feeding at 11.6149 x10^{-4}L/s. The feeding is stopped and reactants are consumed for the remaining time. In Figure 11,12 and 13, the comparison between three feeding policies are shown.

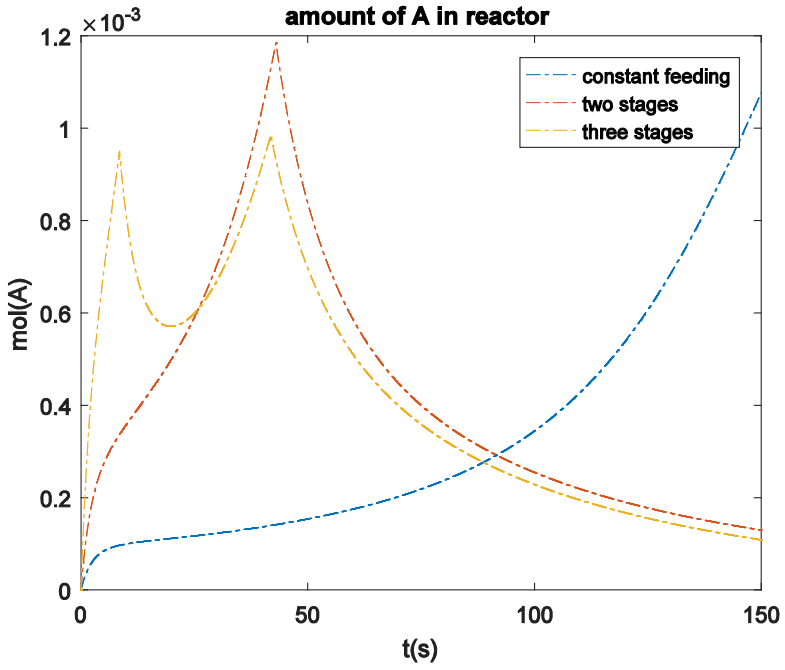

Figure 11. Trajectory of species A with optimal (a) constant feeding policy (b) two stages feeding policy (c) three stages feeding policy

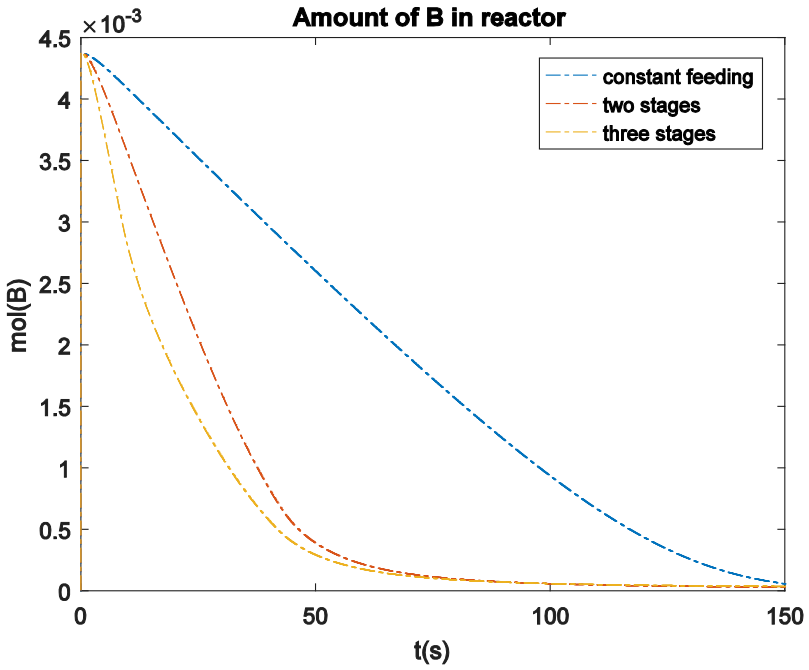

Figure 12. Trajectory of species B with optimal (a) constant feeding policy (b) two stages feeding policy (c) three stages feeding policy

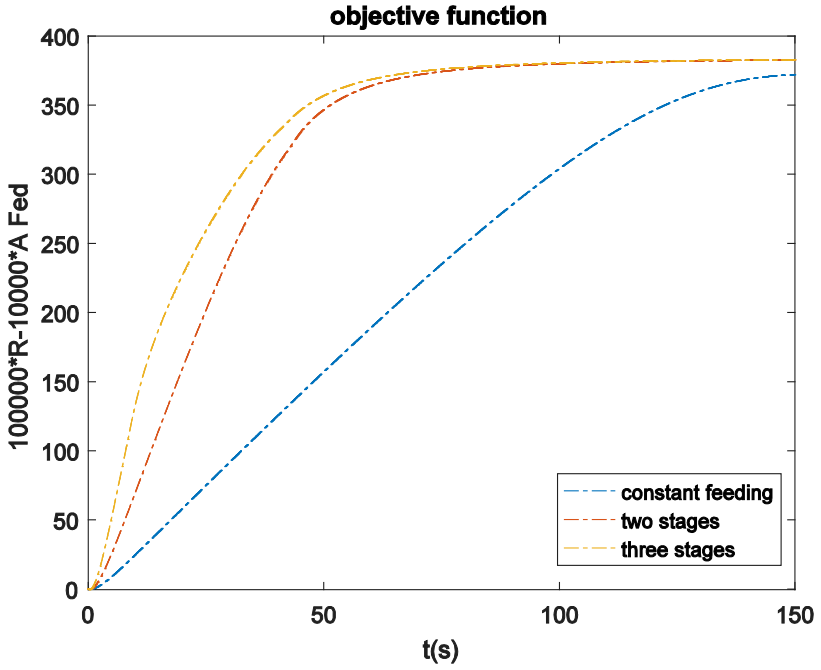

Figure 13. Trajectory of objective function with optimal (a) constant feeding policy (b) two stages feeding policy (c) three stages feeding policy

Chapter 6. Conclusions

We developed a model to study single phase mixing process in a stirred tank reactor driven by a Rushton turbine and a pitched blade impeller. Based on CFD simulations and finite volume discretization method, a CFD-based compartmental model is built. To characterize mixing performance, a benchmark reaction system is integrated. The model is validated by a resolution sensitivity test and the best resolution for discretization is determined. With the developed model, optimization problems were defined and solved to find the best operating policy. First a static operating policy which feed reactants in a constant rate was studied. In this problem we solve for the best addition point and addition rate that maximize the yield with least reactants fed. To solve this optimization problem, mixed-integer surrogate optimization algorithm is adopted and the best static operating policy is determined. Noticing that a constant feeding rate will lead to accumulation of reactants at the end of process which result in significant waste, dynamic operating policies are considered. Instead of feeding in a constant rate, the whole process is broken into several feeding stages and different feeding rate is adopted at different stages. By determining the time span and feeding rate at each feeding stage, the optimal dynamic operating policy is solved. Interior point method is adopted to solve for the optimizer and significant improvement from constant feeding rate is achieved. Using this framework, we can find the optimal operating policy for reactors where imperfect mixing presents.

References

1. Cheng, D., et al., *Modelling and experimental investigation of micromixing of single-feed semi-batch precipitation in a liquid–liquid stirred reactor.* Chemical Engineering Journal, 2016. **293**: p. 291-301.
2. Levenspiel, O. and C. Levenspiel, *Chemical reaction engineering*. Vol. 2. 1972: Wiley New York etc.
3. Guha, D., et al., *CFD-based compartmental modeling of single phase stirred-tank reactors.* AIChE Journal, 2006. **52**(5): p. 1836-1846.
4. Duan, X., et al., *Numerical simulation of micro-mixing in stirred reactors using the engulfment model coupled with CFD.* Chemical Engineering Science, 2016. **140**: p. 179-188.
5. Fox, R.O. and H.L. Stiles, *Computational models for turbulent reacting flows*. Vol. 419. 2003: Cambridge university press Cambridge.
6. Mehta, R.V. and J.M. Tarbell, *Four environment model of mixing and chemical reaction. Part II. Comparison with experiments.* Aiche Journal, 1983. **29**(2): p. 329-337.
7. Baldyga, J. and J.R. Bourne, *A fluid mechanical approach to turbulent mixing and chemical reaction part I Inadequacies of available methods.* Chemical Engineering Communications, 1984. **28**(4-6): p. 231-241.
8. David, R. and J. Villermaux, *Interpretation of micromixing effects on fast consecutive competing reactions in semibatch stirred tanks by a simple interaction-model.* Chemical Engineering Communications, 1987. **54**(1-6): p. 333-352.
9. Nienow, A.W., et al., *A new pair of reactions to characterize imperfect macro-mixing and partial segregation in a stirred semi-batch reactor.* Chemical Engineering Science, 1992. **47**(9–11): p. 2825-2830.
10. Rahimi, M. and R. Mann, *Macro-mixing, partial segregation and 3-D selectivity fields inside a semi-batch stirred reactor.* Chemical Engineering Science, 2001. **56**(3): p. 763-769.
11. Mann, R., P.P. Mavros, and J.C. Middleton, *A structured stochastic flow model for interpreting flow-follower data from a stirred vessel.* Transactions of the Institution of Chemical Engineers, 1981. **59**(4): p. 271-278.
12. Rahimi, M., P.R. Senior, and R. Mann, *Visual 3-D modelling of stirred vessel mixing for an inclined-blade impeller.* Chemical Engineering Research & Design, 2000. **78**(A3): p. 348-353.
13. Vicum, L., et al., *Multi-scale modeling of a reactive mixing process in a semibatch stirred tank.* Chemical Engineering Science, 2004. **59**(8-9): p. 1767-1781.
14. Wang, Z., et al., *Simulation of barium sulfate precipitation using CFD and FM-PDF modeling in a continuous stirred tank.* Chemical Engineering & Technology, 2007. **30**(12): p. 1642-1649.
15. Liu, Y. and R.O. Fox, *CFD predictions for chemical processing in a confined impinging-jets reactor.* Aiche Journal, 2006. **52**(2): p. 731-744.
16. Han, Y., et al., *Numerical simulation on micromixing of viscous fluids in a stirred-tank reactor.* Chemical Engineering Science, 2012. **74**: p. 9-17.

17. Uebel, K., et al., *CFD-based multi-objective optimization of a quench reactor design.* Fuel Processing Technology, 2016. **149**: p. 290-304.
18. Foli, K., et al., *Optimization of micro heat exchanger: CFD, analytical approach and multi-objective evolutionary algorithms.* International Journal of Heat and Mass Transfer, 2006. **49**(5-6): p. 1090-1099.
19. Elsayed, K. and C. Lacor, *Modeling and Pareto optimization of gas cyclone separator performance using RBF type artificial neural networks and genetic algorithms.* Powder Technology, 2012. **217**: p. 84-99.
20. Duchaine, F., T. Morel, and L.Y.M. Gicquel, *Computational-Fluid-Dynamics-Based Kriging Optimization Tool for Aeronautical Combustion Chambers.* Aiaa Journal, 2009. **47**(3): p. 631-645.
21. Vicum, L. and M. Mazzotti, *Multi-scale modeling of a mixing-precipitation process in a semibatch stirred tank.* Chemical Engineering Science, 2007. **62**(13): p. 3513-3527.
22. Cheng, J.C., C. Yang, and Z.S. Mao, *CFD-PBE simulation of premixed continuous precipitation incorporating nucleation, growth and aggregation in a stirred tank with multi-class method.* Chemical Engineering Science, 2012. **68**(1): p. 469-480.
23. Zhao, W., et al., *Application of the compartmental model to the gas-liquid precipitation of CO2-Ca(OH)2 aqueous system in a stirred tank.* AIChE Journal, 2017. **63**(1): p. 378-386.
24. Woo, X.Y., et al., *Simulation of mixing effects in antisolvent crystallization using a coupled CFD-PDF-PBE approach.* Crystal Growth & Design, 2006. **6**(6): p. 1291-1303.
25. Yang, C. and Z.S. Mao, *Numerical Simulation of Multiphase Reactors with Continuous Liquid Phase*. Numerical Simulation of Multiphase Reactors with Continuous Liquid Phase. 2014, San Diego: Elsevier Academic Press Inc. 1-309.
26. Eymard, R., T. Gallouët, and R. Herbin, *Finite volume methods.* Handbook of Numerical Analysis, 2000. **7**: p. 713-1018.
27. Fogler, H.S., *Elements of chemical reaction engineering.* 2016.
28. Land, A.H. and A.G. Doig, *An Automatic Method of Solving Discrete Programming Problems.* Econometrica, 1960. **28**(3): p. 497-520.
29. Jones, D.R., M. Schonlau, and W.J. Welch, *Efficient global optimization of expensive black-box functions.* Journal of Global Optimization, 1998. **13**(4): p. 455-492.
30. Gutmann, H.M., *A radial basis function method for global optimization.* Journal of Global Optimization, 2001. **19**(3): p. 201-227.
31. Holmstrom, K., *An adaptive radial basis algorithm (ARBF) for expensive black-box global optimization.* Journal of Global Optimization, 2008. **41**(3): p. 447-464.
32. Müller, J., *MISO: mixed-integer surrogate optimization framework.* Optimization and Engineering, 2015. **17**(1): p. 177-203.
33. Muller, J., C.A. Shoemaker, and R. Piche, *SO-MI: A surrogate model algorithm for computationally expensive nonlinear mixed-integer black-box global optimization problems.* Computers & Operations Research, 2013. **40**(5): p. 1383-1400.

34. Wang, Z.L. and M. Ierapetritou, *A novel feasibility analysis method for black-box processes using a radial basis function adaptive sampling approach.* Aiche Journal, 2017. **63**(2): p. 532-550.